

Experimental Study on Behaviour of Steel Fibre-Reinforced Beam-Column Joints by Varying the Reinforcement Pattern

P. Balakumar

Assistant professor, PSG institute of technology and applied research, Coimbatore.

J. V. Ramasamy

Professor, Department of Civil Engineering, PSG College of Technology, Coimbatore.

MS. S. Sharmila

Assistant Professor (sr.gr), Department of Civil Engineering, PSG College of Technology, Coimbatore-04

Abstract- In this study, seismic behavior of exterior (T) and corner (L) beam-column joints with conventional reinforcement detailing in the joint region as well as beam-column joints with different anchorage patterns was investigated. The behaviour of specimen with conventional reinforcement pattern (CS-T & CS-L) in the joint region is compared with TS-A, TS-B, LS-A and LS-B. TS-A and LS-A indicate specimen with four inclined bars that extend from column to beam, two from the column portion above the joint and two from the column portion below the joint. TS-B and LS-B are the specimens with four bars in beam, two at top and two at bottom which were intersected to form 'X' shape, provided with round hook anchorage. Steel fibres are included by 1.5% by volume to study the impact of steel fibres in enhancing the performance of beam column joints. These specimens are indicated as CSF-T, TSF-A, TSF-B, CSF-L, CSF-A, CSF-B. The performances of these 12 specimens are compared in terms of lateral load-displacement hysteresis loop, maximum moment capacity, maximum shear capacity, load ratio, energy dissipation capacity and crack pattern. In this paper the comparison of performances of CS-T, TS-A, TS-B and CSF-T are presented.

Keywords: Seismic behavior, Hysteresis, energy dissipation, load ratio.

1. INTRODUCTION

Earthquakes that occurred recently have demonstrated that even when the beams and columns in a reinforced concrete frame joint remain intact, the integrity of the structure is undermined if beam column connection fails. A good seismic performance of beam-column joint depends on the detailing of beam longitudinal reinforcement and confinement in joint [1]. The emphasis of the present study is the evaluation of the seismic performance of exterior joints and corner joints having different anchorage patterns of

beam longitudinal reinforcement and joint transverse reinforcement [8][10]. Since normal concrete is brittle in nature which may also additionally propagate collapse in structural members not designed and detailed in seismic areas during earthquakes. Addition of steel fibres may bridge the cracks increasing the tensile strength of the concrete hence may improve ductility in the members. Therefore a considerable improvement in tensile strength and higher ultimate strain can be obtained. Many researches have been conducted to investigate the flexural behaviour of steel fibre reinforced beam-column joints, such as using steel fibre to replace the lateral reinforcement in the plastic hinges of beam-column joints. Based on the improvement in bond between rebars and concrete after using steel fibers, it is reported that the steel fibers are capable of increasing the anchorage capacity of hooked rebars embedded in the beam-column joints. Steel fibers are well recognized for the ability to enhance the flexural strength, shear strength, fracture toughness, and better energy dissipation capacity. Steel fibers can act also as crack arrester, which delays the dilation of concrete and prevents the development of cracks thereby suppressing a brittle shear failure in favour of more ductile behavior.

Daniel P. Abrams [2] constructed eighteen reinforced concrete beam-column assemblies at small, medium, or large scales (one-twelfth, one-quarter, or three-quarter scales) and concluded that force-deflection relations for one-quarter scale specimens were similar to those of large scale specimens. Juncichro Niwa [6] conducted experiment on eight numbers of one-sixth scaled model specimens that include four T-joint and four knee-joint specimens. The control specimens were casted with , the amount of steel rebars and their arrangements resembling configuration of the rigid-framed railway bridge in Japan [7][9]. Other Specimens were casted and tested with steel fibres varying from 0, 1.0, and 1.5% by volume. The following points are concluded from experimental results of the specimens ; performance of the control specimens and specimens with 1.5% of steel fibers and reduced steel rebars was comparable. Oh [9] reported that the addition of 2% of steel fibers in concrete increases the flexural strength of lightly

reinforced beams by 1.5 times.

Sundararajan and Asha [11] studied the seismic behavior of exterior beam-column joints with square spiral confinement in the joint region along with different reinforcement detailing for anchorage of beam bars and confinement in joint. They

concluded that the different reinforcement detailing improves the seismic performance of the beam- column joints. The main objective of this study is to understand the mechanical behaviour of steel fibre reinforced concrete beam column joint under monotonic loading.

EXPERIMENTAL INVESTIGATION

2.1 Materials used:

Concrete was made with OPC 43 Grade Cement, river sand and 10 mm crushed aggregate. The quantities of materials per cubic meter of concrete determined as per IS 10262:2009 with mix Proportion 1:2.15:1.96:0.5. The 28th day cube compressive strength of all the specimens was 37.52Mpa. Steel Fibres used in the experimental study is of type hooked end fibres with diameter 0.55m, and length 35mm, the aspect ratio L/D of the specimens considered is 64.

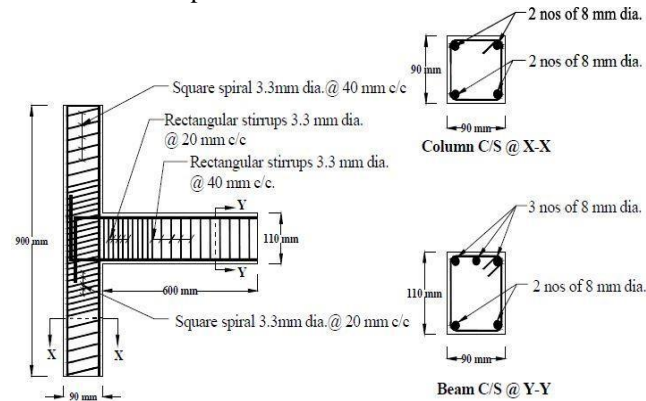


Figure1. Reinforcement detailing of CS-T specimen

2.2 Details of test specimens

The test specimens were 1/4 scale models of typical exterior beam-column joints made up of a single column with one beam in the longitudinal direction (Fig.1). All specimens were cut at mid height of supporting column and at midspan of beams. The specimens were designed for both gravity loads and earthquake forces. The specimens were designed for seismic forces and detailed as per IS 13920-1993.

TS-A and LS-A have four numbers of inclined bars that extend from column to beam, two bars extending from the column portion above the joint and two bars from the column portion below the joint. TS-B and LS-B have four bars in beam, two at top and two at bottom which were intersected to form „X“ shape (Fig. 2).

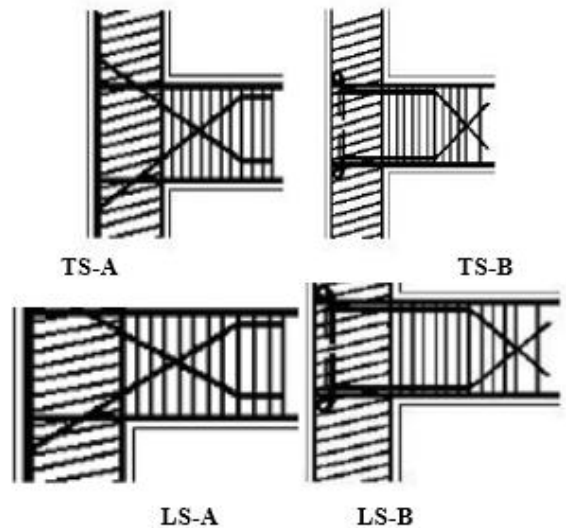


Fig. 2. Various schemes of reinforcement detailing

2.3 Casting and Curing

A total of 12 beam columns specimens were casted for this study as shown in Fig.3. Table 1 and Table 2 give the specifications of the specimens with exterior and corner joints respectively.

Table 1 Specimen specifications – Exterior Joint

Name	Specifications
CS-T	Control specimen with conventional reinforcement pattern
CSF-T	CS –T with steel fibres
TS-A	Specimen with reinforcement pattern A
TS-B	Specimen with reinforcement pattern B
TSF-A	TS-A with steel fibres
TSF-B	TS-B with steel fibres

Table 2. Specimen specifications – Corner Joint

Name	Specifications
CS-L	Control specimen with conventional reinforcement pattern
CSF-L	CS –L with steel fibres
LS-A	Specimen with reinforcement pattern A
LS-B	Specimen with reinforcement pattern B
LSF-A	LS-A with steel fibres
	LS-B with steel fibres

Fig. 3 Casting and Curing of specimens

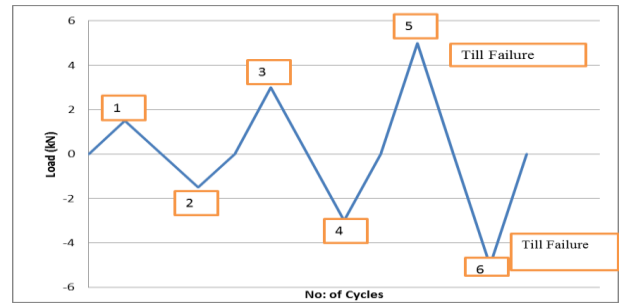


Fig. 5 Cyclic load variation

2.4 Testing arrangement and loading

The specimens were tested under quasi- static loading with the column portion vertical in a 40 ton reaction frame as shown in Fig.4. A constant axial load of 15kN is applied on the column and quasi-static loading is applied at beam tip in six cycles. No axial compression was applied to the columns in order to evaluate a worst-case scenario for the joint core. Hydraulic jacks were placed on top and bottom of beam by for alternate cycle of loading. Proving rings were attached to screw jacks which were used to measure the load applied to the beam end. A reverse cyclic controlled loading is applied on the free end of the beam. Linear variable displacement transducers (LVDT) had been used to measure the deflection at free end of the beam.



Fig. 4 Experimental set-up

The maximum load capacity was found to be 6kN theoretically. Loads were applied in six cycles. First cycle is applied from 0-1.5kN in an increment of 0.375kN and unloaded from 1.5-0 kN in a decrement of 0.0.375kN at top. Second cycle is applied from 0- 1.5kN in an increment of 0.375 kN and unloaded from 1.5-0 kN in a decrement of 0.375kN at bottom. Similarly third and fourth cycle are loaded and unloaded at top and bottom from 0-3 kN.Fifth and sixth cycle are loaded and unloaded at top and bottom from 0 until failure as shown in (Fig.5) Load deflection plots are plotted for all the specimens.

3.RESULTS AND DISCUSSION

3.1 Hysteresis behavior

The load carrying capacity and From the lateral load-displacement hysteresis loops of specimens, it is observed that all the specimens possessed spindle shaped curves showing TS-A with load carrying capacity of 4.5kN and TS-B with 4.3kN. Whereas the control specimen possesses a load carrying capacity of 4.2 kN. The experimental maximum load of TS-A and TS-B was greater than the experimental maximum load of CS-T by 7.14% and 2.4% respectively. CSF-T has 19% higher load carrying capacity with maximum load carrying capacity of 5KN. Fig.6 and Fig 7. Show the hysteresis loops of the specimens.

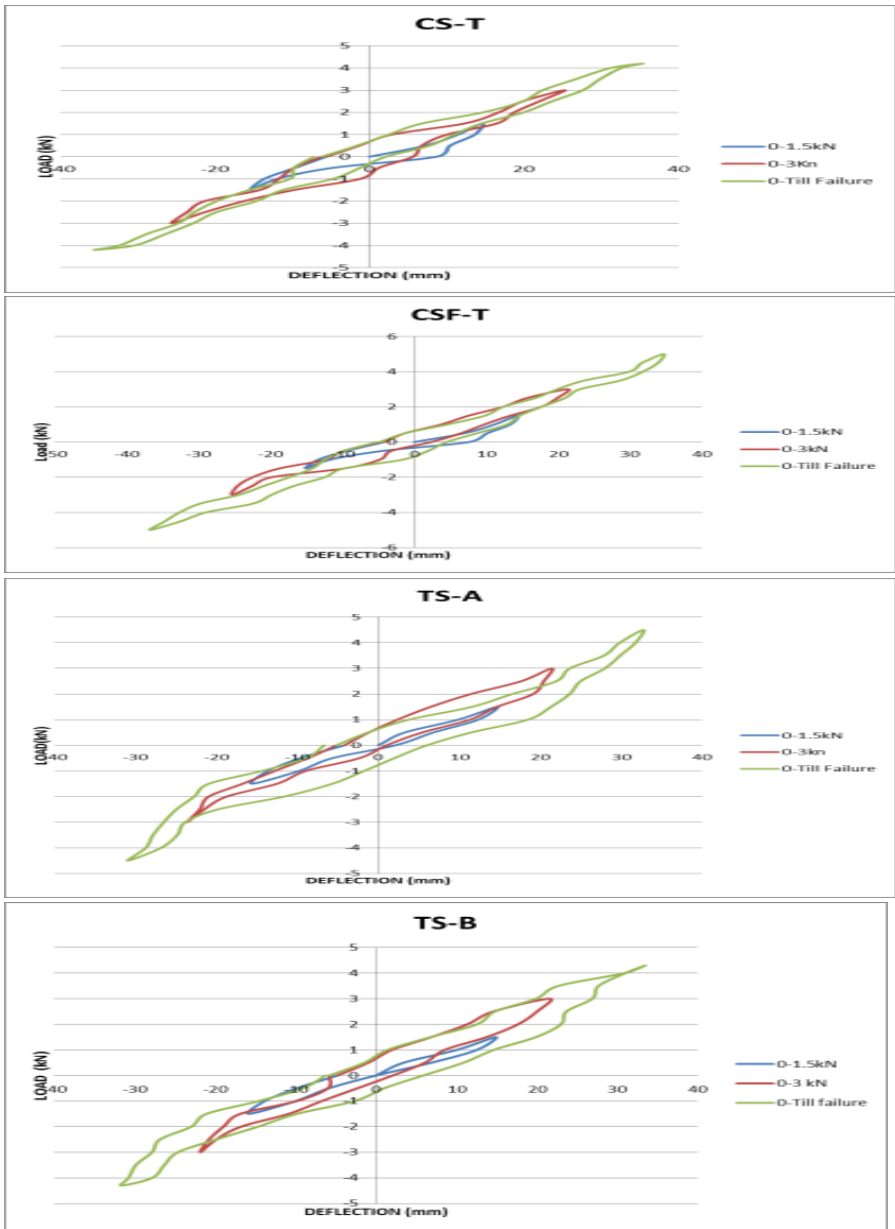


Fig. 6 Hysteresis loop for exterior joint specimens

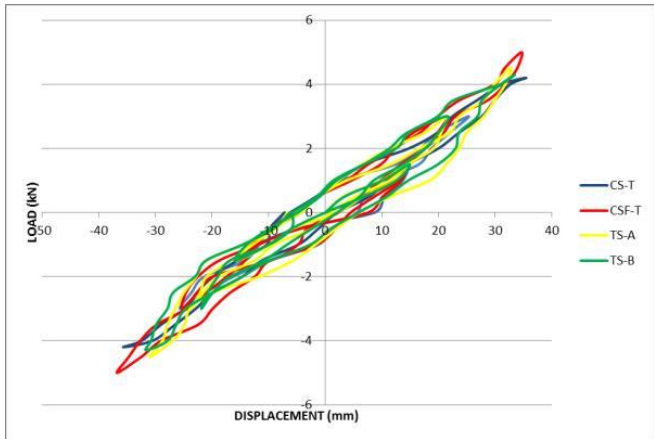


Fig.7 Hysteresis loops of various specimens

3.2 Maximum Moment Capacity

The Maximum Moment Capacity of CS- T,TS-A and TS-B are 2.52 kNm ,2.7 kNm, 2.58kNm respectively. Thus TS-A and TS-B have 7.1% and 2.4% higher moment capacity than CS-T. However the control specimen with steel fibres CSF- T has 19 % higher moment capacity with the value of 3kNm.

3.2 Maximum Shear Capacity

Shear capacity of various joints has been calculated. Joint shear capacity is calculated using the following formulas

$$JS = M \times 10^6 \div (0.9 \times D \times 0.083 \times \sqrt{f_c'} \times h \times b_j)$$

M = Moment at failure in KN-m D = Overall depth of beam in mm

f_c' = 0.8 x compressive strength of concrete at 28 days in N/mm²

h = depth of column in mm

b_j = width of beam in joint portion in mm

Maximum Shear Capacity of CS-T,CSF-T, TS-A and TS-B are 6.91Kn,8.23kN, 7.41kN and 7.07kN respectively CSF-T, TS-A and TS-B have 19% 7.2 % and 2.3%higher shear capacity than CS- T respectively .

Energy dissipation capacity

The effectiveness of any detailing scheme is in the amount

of energy dissipated by the structural component provided with such a detailing scheme. The energy dissipated during a particular loading cycle is computed as the area enclosed within the load versus displacement curve, starting and ending with a zero displacement .From the cumulative energy versus displacement curves of specimens plotted in Figure 6, it is seen that the specimen TS-A has the highest value of E_t of 42 kNmm followed by TS-B with 40 kNmm. E_T of TS-A is 40% higher than that of CS-T whose value 30 kNmm and E_t of TS-B is 33.33% higher. Inclusion of steel fibres increases the Energy Dissipation capacity of the control specimen by 65.33%

Load ratio

To examine the ability of each specimen to maintain its yield load-carrying capacity in the post elastic range, load ratio is calculated which is defined as ratio between the average maximum load and the yield load of the specimen. Load ratio of CS-T, CSF- T,TS-A and TS-B are 2.8, 3.33,3 and 2.86 respectively. Thus CSF-T, TS-A,TS-B have 19%, 7.14% and 2.1% higher yield load carrying capacity than CS-T. These results are tabulated in Table 3.

Table 3 Experimental Results

	CS-T	CSF-T	TS-A	TS-B
LoadCarrying capacity (kN)	4.2	5	4.5	4.3
Moment Capacity(kNm)	2.52	3	2.7	2.58
Shear Capacity (kN)	6.91	8.23	7.47	7.07
Energy Dissipation Capacity (kNmm)	30	49.6	42	40
Load Ratio	2.8	3.33	3	2.86

Crack Pattern

The crack pattern and location provide a first hand insight of the behaviour of the specimen. CS-T experienced minor damage in joint region due to shear cracks [Fig. 8(a)].TS-A failed due to slippage of column and beam bars. [Fig.8(b)]. TS-B experienced hairline cracks in the joint region and the failure was along shear zone in the beam region[Fig. 8(c)]. In CSF-T cracks were developed at the column face penetrated into the joint core. [Fig. 8(d)].



Fig. 8(a) Failure pattern of CS-T



Fig. 8(b) Failure pattern of TS-A



Fig.8(c) Failure pattern of TS-B



Fig.8(d) Failure pattern of CSF-T

CONCLUSIONS

The following conclusions were made from the present experimental investigation:

- The specimen with reinforcement pattern A possesses higher load carrying capacity of 4.5kN which is 7.14 % greater than that of the control specimen. However inclusion of steel fibres increases the load carrying capacity by 19.2%
- Due to the new reinforcement pattern -A, the moment capacity is increased by 7.1% and shear capacity is increased by 7.2%.

Steel fibres increase the moment capacity and shear capacity by 19%.

- The increase in effectiveness of the new detailing scheme -A is proved by the amount of energy dissipated which is 40% higher than the conventional reinforcement pattern and for pattern B it is 33.33% higher. Inclusion of steel fibres increases the Energy Dissipation capacity by 65.33%
- The new reinforcement pattern A has 7.14% higher yield load carrying capacity than the conventional one which shows better performance of the new detailing in post elastic period. Fibre reinforced specimen's exhibit further higher yield load capacity of 19%.
- The specimen with reinforcement detailing pattern A exhibit higher efficiency of seismic behavior than control

specimen and TS-B. Inclusion of steel fibres proved to be successful in further enhancing the seismic behavior as well as reducing crack propagations in beam-column joints.

ACKNOWLEDGEMENT

The authors wish to thank Dr.K Prakasan , Principal incharge, Dr. M Planikumar, Head of the Department of Civil Engineering, PSG College of Technology for providing the necessary facilities and guidance to complete the work successfully.

REFERENCES

- [1] IS: 1893(Part 1): 2016 "Criteria for Earthquake Resistant Design of Structures", Part-1 General Provisions and Buildings, Fifth Revision, Bureau of Indian Standard, New Delhi, India.
- [2] ALACI, Z. KALITCHIN, M. KANDEVA, F. CIORNEI: Method and Device for the Study of Damping of Environmental Friendly Foam Type Materials. In *J Environ Prot Ecol* 21(4), 1298 (2020)
- [3] SAP 2000 Manual (Version 14), "CSI Getting Started with SAP2000", Computers And Structures, Inc. Berkeley, USA.
- [4] JAGADALE S.H. AND SHELKE N.L.,2016, "Analysis of Various Thicknesses Of Shear Wall With

Opening And Without Opening and Their Percentage Reinforcement”, International Journal of Research in Engineering, Science and Technologies, Vol. 1, pp. 212-218.

[5] BAGHERI B. et al., 2012, “Comparative Study of The Static and Dynamic Analysis of Multi-Storey Irregular Building”, International Scholarly and Scientific Research & Innovation, World Academy of Science, Engineering and Technology Vol:6.

[6] LAVANYA PRABHA, S., GOPALAKRISHNAN, M., NEELAMEGAM, M.: Development of high-strength nano-cementitious composites using copper slag, ACI Materials Journal, 2020, 117(4), pp. 37–46.

[7] MOHAN, A , VIJAYAN, D.S. , REVATHY, J., PARTHIBAN, D., VARATHARAJAN, R.: Evaluation of the impact of thermal performance on various building bricks and blocks: A review, Environmental Technology and Innovation, 2021, 23, 101577(2021)

[8] M. THOLKAPIYAN, A.MOHAN, VIJAYAN.D.S: A survey of recent studies on chlorophyll variation in Indian coastal waters, IOP Conf. Series: Materials Science and Engineering 993 (2020) 012041, 1-6.

[9] AJAY HIRAPARA, DHANANJAY PATEL, 2017, “Analysis Of Light Weight Formers In Concrete Slabs Using Voids” International Journal of Advance Engineering and Research Development (IJAERD) Volume 4, Issue 4.

[10] AWADH EWAYED AJEEL, TAMARA ADNAN QASEEM, SALWA RAHMAN RASHEED,2018, “Structural behavior of voided reinforced concrete beams under combined moments” Civil and Environmental Research Vol.10,No:1.

[11] GEE-CHEOL KIM, JOO-WON KANG, 2012, “Calculation of Voided Slabs Rigidities” International Journal of Civil and Environmental Engineering Vol:6, No:5.

[12] JOO-HONG CHUNG, HYUNG-SUK JUNG, BAEK-IL BAE, CHANG-SIK CHOI AND HYUN-KI CHOI, 2018, “Two-Way Flexural Behavior of Donut-Type Voided Slabs” International Journal of Concrete Structures and Materials.

[13] THAAR S. AL-GASHAM, ALI N. HILO, MANAL A. ALAWSI 2019, “Structural behavior of reinforced concrete one-way slabs voided by polystyrene balls” Case Studies in Construction Materials, Vol 11.

[14] GOPALAKRISHNAN, R., MOHAN, A., SANKAR, L. P., & VIJAYAN, D. S. (2020). Characterisation On Toughness Property Of Self-Compacting Fibre Reinforced Concrete. In Journal of Environmental Protection and Ecology (Vol. 21, Issue 6, pp. 2153–2163).

[15] LAVANYA PRABHA, S., DATTATREYA, J.K., NEELAMEGAM, M., SESHAGIRI RAO, M.V., Investigation of bolted RPC plate under direct tension, Journal of Structural Engineering (Madras), 2009, 36(5), pp. 333–341

[16] MOHAN, A., TABISH HAYAT, M.: Characterization of mechanical properties by preferential supplant of cement with GGBS and silica fume in concrete, Materials Today: Proceedings, 2020, 43, pp. 1179–1189.

[17] DHARMAR, S., GOPALAKRISHNAN, R., MOHAN, A.: Environmental effect of denitrification of structural glass by coating TiO₂, Materials Today: Proceedings, 2020, 45, pp. 6454–6458

[18] CHEONG, K.H. AND LEE, S.C.: “Strength of Retempered Concrete”, ACI Materials J. 90(3), 203-206 (1993)

[19] KIRUTHIKA, C., LAVANYA PRABHA, S., NEELAMEGAM, M.: Different aspects of polyester polymer concrete for sustainable construction Materials Today: Proceedings, 2020, 43, pp. 1622–1625

[20] PRABHA, S.L., SURENDAR, M., NEELAMEGAM, M.: Experimental investigation of eco-friendly mortar using industrial wastes, Journal of Green Engineering, 2019, 9(4), pp. 626–637